

Retina imaging by using compact line scanning quasi-confocal ophthalmoscope

Yi He (何 益)^{1,2,3}, Hao Li (李 昊)^{1,2,3}, Jing Lu (卢 婧)^{1,2}, Guohua Shi (史国华)^{1,2*},
and Yudong Zhang (张雨东)^{1,2}

¹Key Laboratory on Adaptive Optics, Chinese Academy of Sciences, Chengdu 610209, China

²Laboratory on Adaptive Optics, Institute of Optics and Electronics, Chinese Academy of Sciences,
Chengdu 610209, China

³University of Chinese Academy of Sciences, Beijing 100049, China

*Corresponding author: guohua_shi@yahoo.com.cn

Received June 21, 2012; accepted August 8, 2012; posted online December 25, 2012

A compact line scanning quasi-confocal ophthalmoscope (LSO) is presented in this letter. Compared with a conventional scanning laser ophthalmoscope (SLO), the bench-top LSO significantly reduces the size, complexity, and cost of SLO utility with routine use. The LSO uses one moving part to produce high-contrast and high-resolution quasi-confocal images with nearly the same performance as a SLO. The LSO has a moderate field of view ($\sim 10^\circ$), which enables images of the macula, the optic nerve head, and other targets to be obtained more quickly and efficiently. An image of the optic nerve head is taken in a preliminary investigation on human subjects. Individual nerve fiber bundles and vessels are resolved at a shallow depth, with a lateral resolution of nearly 10 μm .

OCIS codes: 110.0110, 170.1790, 170.4460.

doi: 10.3788/COL201311.021101.

Scanning laser ophthalmoscopy (SLO) has become a clinical tool for the diagnosis of retinal function and disease^[1–3]. This imaging technique scans a focused spot on retina horizontally by using a high-speed optical scanner and vertically by using a lower-speed scanner to achieve video-rate images^[4]. To achieve a clear resolution advantage, SLO is most often implemented in a confocal arrangement, wherein a limiting aperture is placed in front of the detector at a focal plane that is conjugate to the retina image plane^[2]. The confocal arrangement yields higher-contrast images with relatively high depth discrimination through the rejection of scattered light from the adjacent layers to the image planes^[2,3].

The SLO is a superior tool for the rapid and continuous acquisition of high-contrast images of the ocular fundus and its structures. The SLO has become a valuable diagnostic tool in the research community^[4,5]. However, video rate synchronization of two scanners increases the complexity of the system, and the conjugate setting degrades light collection efficiency. The SLO requires a dilated pupil to increase the numerical number. The backscattered light is then collected from the entire dilated pupil for high light efficiency. Consequently, SLOs are usually found only at specialized facilities and are used almost exclusively by ophthalmologists partly because of instrument size, cost, and complexity^[4].

Conversely, the line scanning quasi-confocal ophthalmoscope (LSO) uses an anamorphic optical element (e.g., cylindrical lens (CL)) to expand the beam in one dimension on the retina plane. Only one moving scanner is needed to scan the beam in the other dimension. The light from the focused line is descanned and detected by a linear array sensor (LAS). A slit aperture (SA) is placed in front of the detector in conjugate of the retina plane to produce a “quasi-confocal” image. This process is facilitated by the light from the adjacent voxels along

the illuminated line, which mixes with the linear array detector^[6–9]. Thus, the LSO has an approximate confocal advantage in image clarity and contrast compared to the SLO. On the contrary, the following features of the LSO are currently unavailable in commercial SLOs: 1. simplified scanning control and frame grabbing provided by the single moving part; 2. reduced number of optical elements, which results in a short optical path and compact design; 3. absence of a dilation requirement, which enables the LSO to be used in emergency situations and to provide patient comfort; 4. one-dimensional (1D) beam on the retina plane, which makes the LSO inherently safer; 5. 1D scanning, which makes the LSO a high-speed imaging instrument that favors future retinal movement tracking. These advantages facilitate low-cost, easy-to-handle, and compact units that are suitable for hand-held operations^[10,11].

A compact LSO system for retina imaging was designed, constructed, and tested in this letter. Figure 1 shows the unfolded optical layout of the LSO. The entire system was modeled and its theoretical optical performance was characterized by using optical design software (Zemax). A galvanometer-driven scanning mirror (SM, 6230H, Cambridge Corporation) conjugated to the entrance pupil was used to create LSO images by scanning a line created by the CL on the retina. The illuminating objective lenses (SL and OL) were used for pupil relay. Backscattered light from the eye fundus passes through the same optical path as the incoming beam then is focused by the detector objective lens (DO) on a SA, which is conjugated to the line beam on the retina. A LAS (linear array CCD, AVIVA M2 CL 1014, ATMEL) was placed close to the SA to record the intensity of the scattered light for each line beam position. Retinal images were consecutively taken by synchronizing the signal from the LAS and the driving signal of the SM^[12].

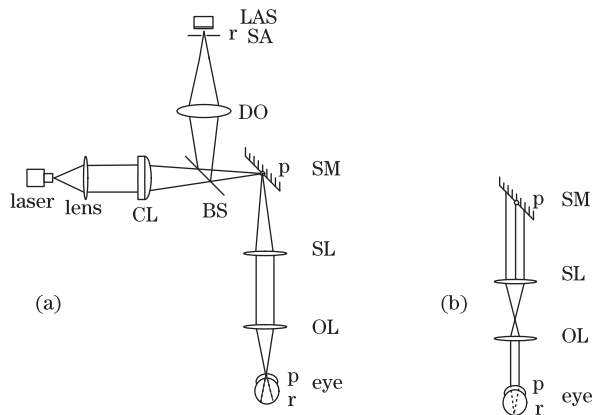


Fig. 1. Unfolded view of the LSO optical path. (a) Side view of the entire system; (b) top view of the illumination path. BS: beam splitter, SL: scan lens, OL: ophthalmoscopic lens, p: pupil plane conjugate, r: retina plane conjugate.

The system is designed to work without the administration of mydriatic agents with a 3-mm pupil. To facilitate patient comfort, a laser diode (LD) with a wavelength of 780 nm was used with an internal objective collimator. The illuminating objective lenses (SL and OL) were optimized and designed to enable the petzval image plane to coincide with the retina plane. This process facilitates good flatness performance. The ZEMAX model analysis shows that a nearly diffraction-limited performance was achieved across a 10° field of view (FOV) (3 mm on the retina plane).

The linear array CCD has 1024 detecting pixels with a $14\text{-}\mu\text{m}$ pitch. This instrument can operate at a maximum data rate of 53 kHz. Therefore, the magnification from the LSO confocal SA (and line-scanning CCD position) to the retina is $\sim 4.7\times$. The transverse airy disk diameter referenced to the retina is $\sim 4.7\text{ }\mu\text{m}$, which corresponds to $22\text{ }\mu\text{m}$ at the detector plane for the magnification used. According to the Zemax design, a $25\text{-}\mu\text{m}$ SA projects to roughly $5.3\text{ }\mu\text{m}$ on the retina or ~ 1.1 times to the airy disc, which is tightly confocal. A $50\text{-}\mu\text{m}$ SA ($\sim 10.6\text{ }\mu\text{m}$ on the retina) is less confocal, allowing more scattered and aberrated light without improving the imaging. Therefore, a larger SA results in lesser LSO confocal. We used a $50\text{-}\mu\text{m}$ SA to the image nerve fiber bundles near the optic nerve head (ONH), then switched to $25\text{-}\mu\text{m}$ SA to obtain a better contrast for the blood vessels.

The LSO imaging performance was characterized by a model eye with a customized resolution chart placed at the retinal conjugate. Figure 2(a) shows the design of the resolution chart. The four rectangular boxes from the inner to the outer layer represent the 1° , 1.5° , 2° , 3° image FOVs, respectively. Two sets of differential resolution target charts in the horizontal and vertical directions are corroded in the central 1° image FOV, and the figures on the target chart represent the linewidth of the targets. All the confocal images in this letter are raw images captured from 30-Hz video with a resolution of 1024×512 pixels. Figure 2(b) shows that the horizontal FOV fills up almost three rectangles of resolution charts, and the inclusion of the marginal area the FOV is $\sim 10^\circ$. Figure 2(c) shows the differential resolution target charts in the central 1° FOV. The $10\text{-}\mu\text{m}$ rectangular lines are clearly visualized. Thus, the lateral resolution

is adequately $10\text{ }\mu\text{m}$. The customized resolution chart is flat, which is different from the curvature of the human retina and the design of our lens, which indicates that the field flatness of the resolution chart is remarkable. However, this result is not observed in the human retina imaging results.

The LSO was then tested on several volunteers under the same condition. The 780-nm power of the illumination wavelength was less than $500\text{ }\mu\text{W}$ or roughly 50 times below the maximum permissible exposure levels for the human eye under the American National Standards Institute (ANSI)^[13]. Figure 3 shows the images of volunteer eyes acquired from the LSO. Good field flatness was ensured compared with those of the resolution chart.

Figure 3(a) shows the image of ONH using a larger $50\text{-}\mu\text{m}$ SA. Individual nerve fiber bundles and vessels at a shallow depth are clearly resolved. However, the LSO is less confocal with a larger SA. Therefore, backscattered light from other layers (e.g., deep layers) is also collected, as evidenced by the bright appearance of the disc.

The LSO achieves better contrast and depth resolution as the SA becomes smaller. Vessels and photoreceptors along the rim can be visualized with a $25\text{-}\mu\text{m}$ SA (Fig. 3(b)). Compared with Fig. 3(a), the contrast in Fig. 3(b) is higher with several visible smaller vessels. For comparison, the main retinal arteries are $\sim 200\text{ }\mu\text{m}$, and the smallest retinal capillaries are 10 to $20\text{ }\mu\text{m}$. Figure 3(c) shows the image of the same eye acquired from a commercial SLO (HRT_{III} Heidelberg Engineering Inc.).

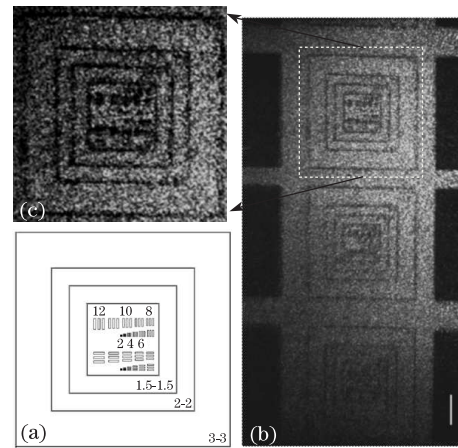


Fig. 2. (a) Resolution chart; (b) image of resolution chart; (c) zoom-in image from image (b). Scale bar = 1 mm.

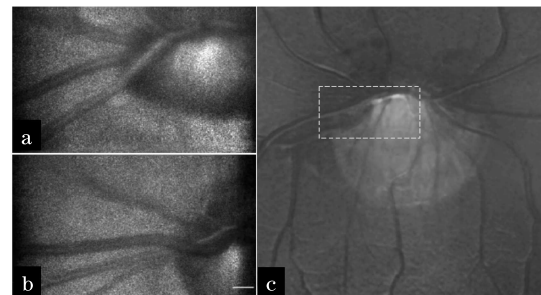


Fig. 3. LSO of the same eye with (a) $50\text{-}\mu\text{m}$ and (b) $25\text{-}\mu\text{m}$ SAs. Horizontal or vertical FOV is $\sim 10^\circ$ and $\sim 5^\circ$, respectively. Scale bar = 1.4 mm. (c) SLO co-added image with registration.

The FOV in Fig. 3(c) is about 30° , and the image is co-added from 64 registered frames. The manufacturer used image processing and color imaging techniques to enhance the contrast and appearance of images. Thus, the raw images in Figs. 3(a) and (b) have a little low contrast. However, compared to Fig. 3(c) the images acquired from the LSO have almost the same resolution.

The speckle artifact in the retina image is due to the use of a LD. Speckle reduction can be achieved by a broad-band light source, such as a superluminescent diode. However, this process is more expensive than a LD. Speckle is not correlated with images. Therefore, digital processing techniques can naturally suppress speckle artifact for applications that require completely minimized speckle artifacts.

A compact LSO was designed and developed for various research and clinical applications. The bench-top LSO instrument significantly reduces the size, complexity, and cost of SLO. The LSO can produce high-resolution retinal images with only one moving part. This feature significantly reduces instrument footprint and the number of optical components. The LSO has a 10° FOV, which allows images of the macula, the ONH, and other targets to be obtained more quickly and efficiently.

In conclusion, the LSO is not intended for current SLO replacement, but rather for the achievement of a nearly equivalent imaging performance in a compact, low-cost unit. The SLO uses a single-point detector, which encodes the image information into temporal variations. Any arbitrary detection aperture size relative to the airy disc can be projected and detected, depending on the relay optic and confocal pinhole size. Unlike the SLO, the minimum resolution of the LSO is constrained by the detection hardware. The Nyquist sampling limit sets the maximum resolvable spatial frequency, which corresponds to twice the pixel separation. Based on the previous discussion of the separation of adjacent pixels and the quasi-confocal line-scanning method, this is a fraction of the airy disc diameter for the production of ideal confocality and diffraction-limited resolution using LSO. However, small pixels relative to the airy disc produces good confocal conditions where light collection efficiency is significantly diminished. Sampling below the airy disc results in rapid loss of signal strength without appreciable resolution improvement. Thus, complexity reduction

slightly diminishes resolution performance. The LSO produces nearly equivalent, quasi-confocal images. The resolution of our initial imaging results is $\sim 10 \mu\text{m}$. Considering its advantages against SLO, the LSO therefore efficiently satisfies our goal.

This work was supported by the National Natural Science Foundation of China (No. 61108082) and the Knowledge Innovation Program of Chinese Academy of Sciences (No. KGCX2-Y11-920). The authors thank Lixin Zhao and Mingyong Chen for their helpful discussions regarding this project.

References

1. R. H. Webb and G. W. Hughes, IEEE Trans. Biomed. Eng. **BME-28**, 488 (1981).
2. R. H. Webb, G. W. Hughes, and F. C. Delori, Appl. Opt. **26**, 1492 (1987).
3. R. H. Webb and D. P. Wornson, "Scanning optical apparatus and method" U. S. Patent 4,768,874 (1988).
4. A. E. Elsner, A. E. Jalkh, and J. J. Weiter, in *Proceedings of Practical Atlas of Retinal Disease and Therapy* 19 (1993).
5. A. E. Elsner, L. Moraes, E. Beausencourt, A. Remky, S. A. Burns, J. J. Weiter, J. P. Walker, G. L. Wing, P. A. Raskauskas, and L. M. Kelley, Opt. Express **6**, 243 (2000).
6. Y. S. Sabharwal, A. R. Rouse, L. Donaldson, M. F. Hopkins, and A. F. Gmitro, Appl. Opt. **38**, 7133 (1999).
7. C. J. R. Sheppard and X. Q. Mao, J. Mod. Opt. **25**, 1169 (1998).
8. T. R. Corle, C. H. Chou, and G. S. Kino, Opt. Lett. **11**, 770 (1986).
9. R. D. Ferguson, "Line-scan laser ophthalmoscope" U. S. Patent 6,758,564 (2004).
10. D. X. Hammer, R. D. Ferguson, T. E. Ustun, C. E. Bigelow, N. V. Iftimia, and R. H. Webb, J. Biomed. Opt. **11**, 041126 (2006).
11. K.-B. Im, S. Han, H. Park, D. Kim, and B.-M. Kim, Opt. Express **13**, 5151 (2005).
12. Y. He, G. Shi, J. Lu, H. Li, and Y. Zhang, Acta Opt. Sin. (in Chinese) **32**, 0117001 (2012).
13. A. N. S. I. (ANSI), *American National Standard for the Safe Use of Laser* 2000, American National Standard Institute, Inc.